

Summary Report on Progress During the First Year

The LAPPD Collaboration

June 29, 2010

1 Introduction

The Large-Area Psec Photo-Detector (LAPPD) Collaboration consists of physicists and engineers at three national labs: Argonne, Fermilab, SLAC; five universities: UC Berkeley (Space Sciences Lab), Chicago, Illinois at Chicago, Illinois Champaign-Urbana, Hawaii, and Washington Univ. at St. Louis; and three small US companies: Arradance, Muons,Inc, and Synkera[1]. The LAPPD is funded by the Department of Energy’s Office of High Energy Physics through the HEP Division of Argonne.

The collaboration was formed to develop large-scale ‘frugal’ photo-detectors capable of mm-scale space resolution and psec-range time resolution for use in particle physics, astrophysics, nuclear sciences, and medical imaging. The goal is to develop commercializable modules within the three year program.

The outline of the report is as follows. The organization of the collaboration is described in Section 2. Section 3 gives a guide to further documentation on the LAPPD web site. Section 4 is a brief summary of the most important technical achievements. The Year One ARRA Milestones are addressed in Section 5. Section 6 gives a brief summary.

The development of very large-area planar, thin, fast, and also economical photo-detectors could prove to be a ‘disruptive technology’ [2] for a wide range of applications in science and industry. Different applications will have different requirements in the parameter space of time and space resolution, area, and cost, to name three of the dimensions of parameter space. One of the requirements of the basic design being developed is that it can be optimized for specific applications. Figure 1 shows our model for working closely with application groups while maintaining focus on the detector development.

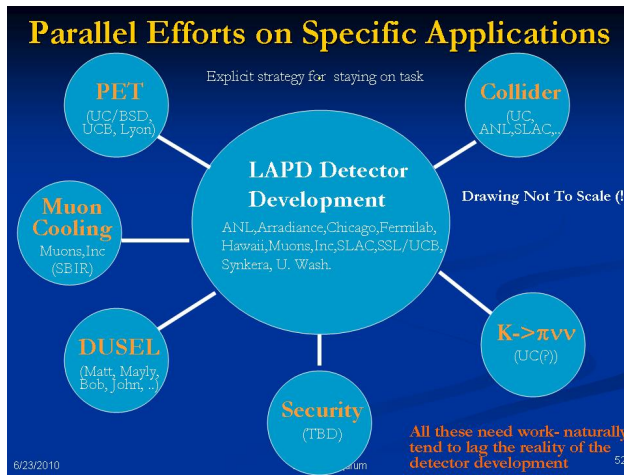


Figure 1: The organizational model for working closely with application groups to understand the requirements and optimize for each application.

Organization Chart

R&D Program for the Development of Large-Area Fast Photodetectors

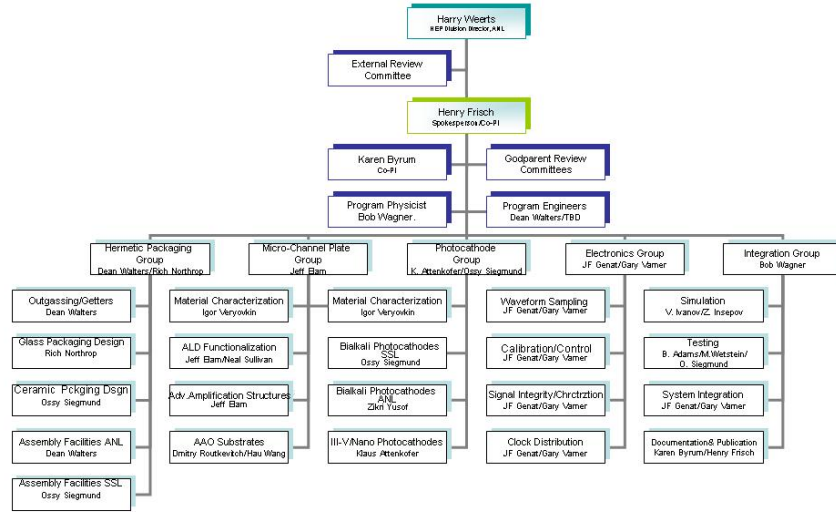


Figure 2: The organization chart for the LAPPD collaboration showing the five major efforts: Hermetic Packaging, Micro-channel Plates, Photocathodes, Electronics, and Integration

2 The Structure of the Collaboration and Effort

The LAPPD organization is shown in Figure 2. There are five related efforts: Hermetic Packaging, Micro-channel Plates, Photocathodes, Electronics, and Integration. The groups have regular weekly teleconferenced meetings; intergroup communication is done through a Blog, a web-based library of images and documents and talks, and a weekly teleconference. Progress is monitored with review panels for the first four of the groups. Each panel consists of four internal experts chosen (generally) from other technical areas in the collaboration, and several outside experts, chosen both for expertise and healthy skepticism.

3 Documentation

The project is heavily documented on the web at <http://psec.uchicago.edu/>. Table 1 gives the links from this page to specific topics.

Main Page	http://psec.uchicago.edu/index.php
Library	http://psec.uchicago.edu/library/index.php
Collaboration members	http://psec.uchicago.edu/people.php
Godparent Committees	http://psec.uchicago.edu/godparents.php
Image Library	http://psec.uchicago.edu/library/sketches/
Document Library	http://psec.uchicago.edu/library/doclib/
Properties of Materials	http://psec.uchicago.edu/library/index.php
Blog (weekly mtg)	https://hepblog.uchicago.edu/cdf/cdf2/
Electronics Blog	https://hepblog.uchicago.edu/psec/psec1/
All Other Topics	http://psec.uchicago.edu/library/index.php

Table 1: Links from <http://psec/web/psec/> to specific LAPPD topics.

4 Technical Achievements and Knowledge Gained

We are just at the end of the first year of the project. Perhaps the hardest achievement has been organizational rather than technical- the creation of a functioning collaboration spanning a wide range of fields that have different cultures and that rarely interact. This has gone more smoothly than we could have predicted. We list some of the highlights below.

4.1 Technical Achievement 1: First Demonstration of Gain, Uniformity, and Lifetime in an ALD-coated Glass-substrate Micro-channel Plate

The left-hand panel of Fig. 3 shows a phosphor screen at SSL following a chevron pair of glass capillary MCP's functionalized by Arradiance. One can see the 'multi' structure of the first plate even through the amplification stage of the second. (The dips at the multi boundaries are accentuated as the pair is measured at lower gain). We measure gains $\geq 10^6$, and adequate ($\sim 10\%$) uniformity at high gain. The right-hand panel shows gain versus charge extracted; even though these particular plates were not vacuum-baked one sees a much faster approach to an acceptable aging behavior than pre-scrubbed commercial plates.

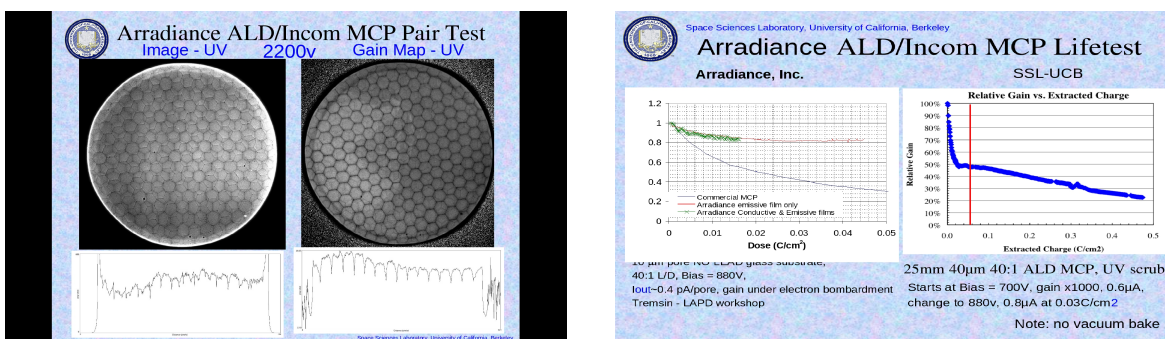


Figure 3: Left: the SSL phosphor screen following a chevron pair of ALD-functionalized glass capillary MCP's. Right: gain versus charge extracted.

Knowledge Gained

Inexpensive glass substrates functionalized by ALD are excellent high-gain planar amplification structures, opening the way for large-area commercial and scientific applications.

4.2 Technical Achievement 2: Detailed Design of the Ceramic-Body 8” MCP-PMT

The SSL group has made a detailed design of a ceramic-body 8”-square MCP-PMT, building on their technical experience in the design of the Planacon and many other successful MCP-PMT designs. Figures 4, 5, 6 and 7 show details of the construction, HV connections, and assembly.



Concept 'A' vs. Concept 'B'

- Concept 'A' (initial design)
 - Anode: Thick-film paste technology on alumina
 - Tube walls: Multi-layer Kovar and alumina sandwich
 - Spacers: Grid-type spacers supporting MCPs/window
- Concept 'B' (simpler design)
 - Anode: Mo-Mn "high temp" technology on alumina
 - Tube walls: Single thick alumina frame with Cu indium well

12 June 2010 J. McPhate - LAPP Collaboration Meeting 2



Modifications to Initial Design: The Anode

- Thick-film technology characteristics
 - Multi-layer conductor/insulator structures (not needed for this anode)
 - LAPP anode size requires 4 screening steps per thick-film layer (vendor's screener is too small)
 - Vias made by "pulling" paste through substrate holes with vacuum (vendor worried about flatness/size of part making this very difficult)
 - Not compatible with hydrogen braze for body seal (requires less standard vacuum braze)
 - Very reliable process that we have used it for many years in other devices (but vendor has significant reservations due to the size of the LAPP anode)
- High-temp Mo-Mn process characteristics
 - One conductive layer only (sufficient for LAPP anode)
 - Mo-Mn materials can be painted by hand (eliminates vendor's screener issue)
 - Vias are sealed with brazed-in pins - no vacuum. Pins allow feedthrough of HV on anode.
 - Compatible with standard belt furnace hydrogen braze
 - Highly reliable process - used for military application (vendor more comfortable with dealing with large anode in this technology)

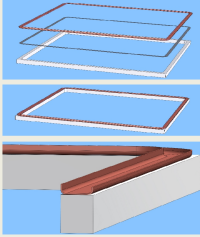
12 June 2010 J. McPhate - LAPP Collaboration Meeting 2

Figure 4: Left: The new concept for the ceramic body being built at SSL. Right: Details of the new concept.

Figure 5 shows details of the new sidewall assembly. The new design has only a single brazed joint compared to the previous many brazes in the Planacon-style design. Figure 5 also shows the details of the getter assembly.



Single Joint Brazed Tube Wall

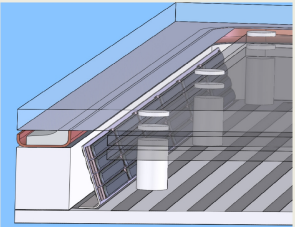


- Much simplified design improves reliability/yield of hermetic seal.
- Ceramic is double ground and machined to shape. Very flat.
- Ceramic cross-section approx 5mm x 7.4mm. Strong foundation.
- Indium cup (seal flange) is compound-die stamped OFHC Cu.

12 June 2010 J. McPhate - LAPP Collaboration Meeting 5
Joined via hydrogen braze at ~850°C



Possible Getter Assembly



- Spot weld SAES getter strips to bent shim
- Getters both sides
- Spot assembly to anode extra ground plane along HV sides (both sides)
- Each assembly accommodates 2x4x6 = 48 getters
- Total of 96 getter strips
- Potential problems
 - Hard to spot "thick" shim to anode
 - Top is poorly restrained - could short MCPs

12 June 2010 J. McPhate - LAPP Collaboration Meeting 11

Figure 5: Left: Details of the new sidewall assembly. Right: Proposed getter details.

Technical Achievement 2 Continued:

The SSL design is quite advanced and builds on their extensive experience building sealed MCP-PMT tubes. Figures 6 and 7 show more assembly details and the assembly flow diagram.

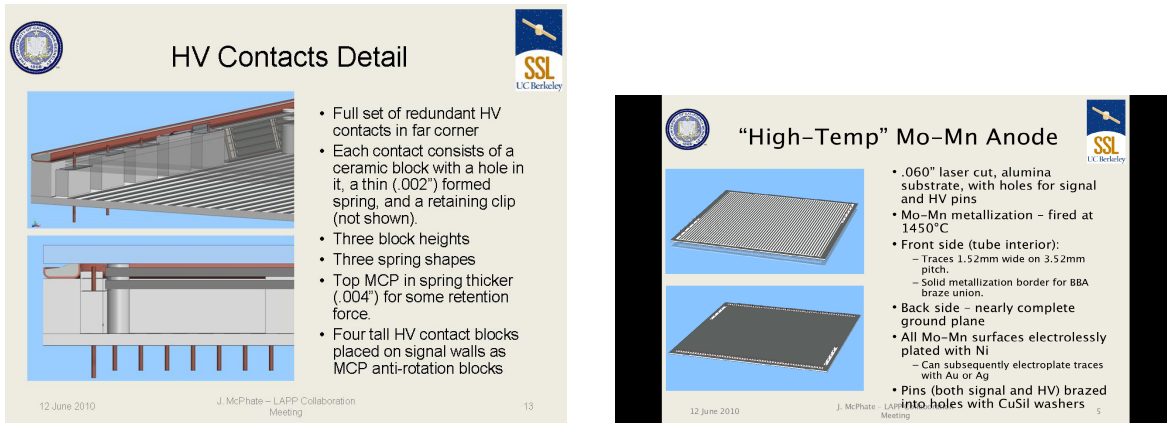


Figure 6: Left: Details of the HV connections. Right: Details of the anode.

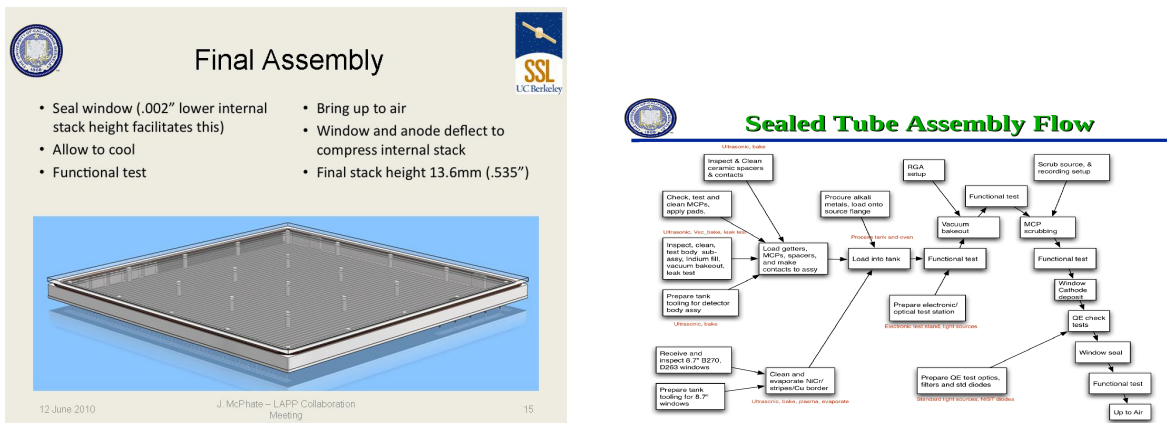


Figure 7: Left: The final assembly of the SSL ceramic sealed tube. Right: the assembly flow diagram.

Knowledge Gained

Techniques and procedures for extending the successful long-time technology used in the Planacon MCP-PMT's and NASA flights to larger-areas and more economical designs, while retaining the strengths of tested designs.

4.3 Technical Achievement 3: Design and Construction of the Assembly Facility for the Ceramic-Body 8" MCP-PMT

The facilities at SSL are in the process of being upgraded to handle the 8"-square ceramic-body MCP-PMTs. The left-hand panel of Fig. 8 shows the design of the large chamber for the assembly of 8" MCP-PMT's. The right-hand panel gives a summary of the status of the facilities for both the prototype size (left-hand columns) and 8" size (right-hand columns).

All the necessary facilities for the prototype-type size are complete. All the design and preparatory work for the 8" module also is complete, with all parts either in fabrication or out for bid. Figure 9 shows the plan and status for the large photocathode chamber of the assembly facility.



Figure 8: Left: The design of the large chamber for the assembly of 8" MCP-PMT's. Right: A summary of the status of the facilities for both the prototype-type size (left-hand columns) and 8" size (right-hand columns).

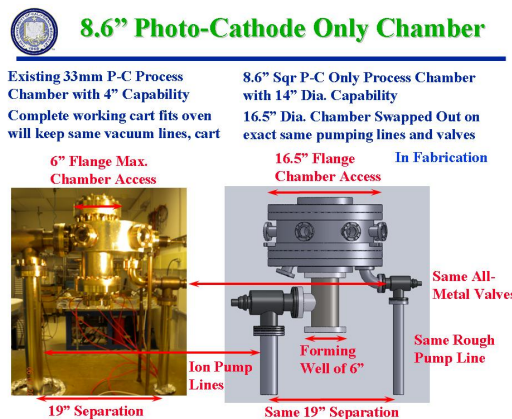


Figure 9: The plan and status for the large photocathode chamber of the assembly facility.

Knowledge Gained

Costs of large vacuum tanks and assembly facilities, which will be relevant to the cost of a production facility. We find from the low bids that these have dropped dramatically compared to 10 or more years ago due to changes in technology and material science.

4.4 Technical Achievement 4: Integrated Mechanical Design for a Frugal 16” by 24” Glass Photodetector Supermodule

Figure 10 shows a mock-up using real parts of the all-glass ‘Frugal’ Supermodule, consisting of six 8”-square Tiles with a common readout. The Tiles are sealed vacuum tubes, with transmission-line anodes in an ‘Inside-Out’ configuration in which the anode strips are electrically connected together and to ground at DC, but act as one side of a 50-ohm transmission line at the (RF) frequencies of the MCP rise-times.



Figure 10: The ‘Frugal’ 16” by 24” Glass Photodetector Supermodule, consisting of six 8”-square Tiles with a common readout.

The side-view of the SuperModule is shown in the left-hand panel of Fig. 11. The ‘Inside-Out’ construction of the anode transmission lines and connection to the waveform sampling chips is shown in the right-hand panel. This configuration has been fabricated and has been measured with a network analyzer, fast pulser, and scope. Simulation is underway with Ansoft and SimIon packages. We have gotten bids on all the parts of this construction in quantities ranging from 10 to 10,000 pieces. It seems frugal, at least so far.

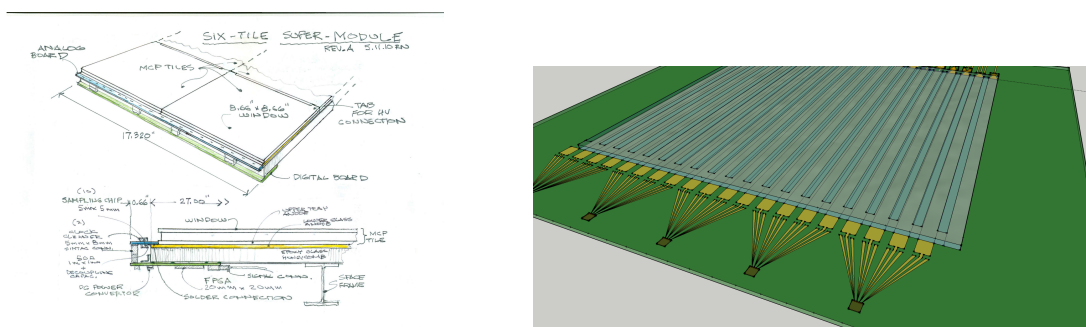


Figure 11: Left: A sketch of the SuperModule showing the side-view. Right: The ‘Inside-Out’ construction of the anode transmission lines and connection to the waveform sampling chips

Knowledge Gained

Costs of constructing large panels. Mechanical integration of analog front-end and digital data acquisition system. Validation of the grounded anode (‘Inside-Out’) scheme.

4.5 Technical Achievement 5: Construction of an Hermetic 8"-square glass tile MCP-PMT body.

The first glass 8"-square Tile prototype outer assembly is shown in Fig. 12. This prototype incorporates the real pieces for sidewall, silvered anode bottom plate, and window, and is hermetically sealed top and bottom with a matched Schott frit. A pump-out port is attached at the upper right for vacuum tests; the final tile will be assembled in vacuum and will not have any external penetrations of the sidewall.



Figure 12: The first glass 8"-square Tile prototype outer assembly (body). This prototype incorporates the real pieces for sidewall, silvered anode bottom plate, and window, and is hermetically sealed top and bottom with frit.

Knowledge Gained

It is possible to make hermetic seals of a large-area thin planar vacuum package using inexpensive Pyrex glass. Very frugal anode strips can be made by silk-screening silver paste on glass. Seals can be made over the silver anode strips.

4.6 Technical Achievement 6: A Unified Design of the RF Signal and DC HV Electrical Paths for a Large-Area Planar ALD-Functionalized Geometry

The electrical circuit of the photo-detector must provide for a DC path for the HV, including capacitive bypassing to diminish the commonly-seen ringing and after-pulsing, and a low-inductance 50-ohm path to the front-end digitization. The right-hand panel of Figure 13 shows the proposed solution. Note that the tiles have no penetrations through the vacuum walls; all signal transmission is done capacitively, and the HV and Ground are applied externally through the silver layer on the window and anode, respectively. The design thus allows custom tiling of different geometries with a single tile design.



Figure 13: Left: The ‘stack-up’ of the tile. Gap 1 is at the top (photocathode to MCP1-In), and Gap 3 is at the bottom (MCP2-Out to Anode). The high voltage is connected externally at the top of the sidewall on the silk-screened window pattern ; the (DC) ground is connected externally to the bottom of the sidewall on the silk-screened anode pattern. Right: The equivalent electrical circuit of the photo-detector.

Knowledge Gained

An economical design capable of high bandwidth, front-end impedance matching, local DC current sources, capacitive bypassing, and good mechanical sealing surfaces, with no pins penetrating the vacuum envelope.

4.7 Technical Achievement 7: Development of New Resistive Coatings for Micro-channel Plates

In addition to the pioneering work by the Arradiance group on functionalizing MCP plates (see Technical Achievement 4.1), the Argonne ALD group has successfully made working MCP's by functionalizing glass capillary plates with a resistive layer followed by an emissive layer. The group has now developed new resistive layers with better characteristics than AZO [3]. Figure 14 describes the advantages and current status (left-hand panel), and shows measurements of reproducibility (right-hand panel).

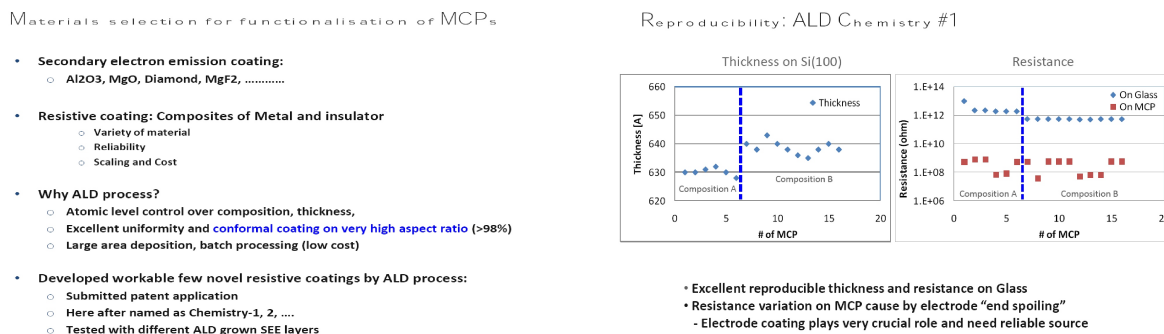


Figure 14: Left: Advantages of ALD and current status of the ANL ALD effort. Right: Measurements of reproducibility.

The left-hand panel in Figure 15 shows the resistivity curve of one of these new formulations. Resistivity is plotted versus the number of ALD metal cycles. The right-hand panel shows measurements of uniformity on a large substrate, a step towards industrial scale-up.

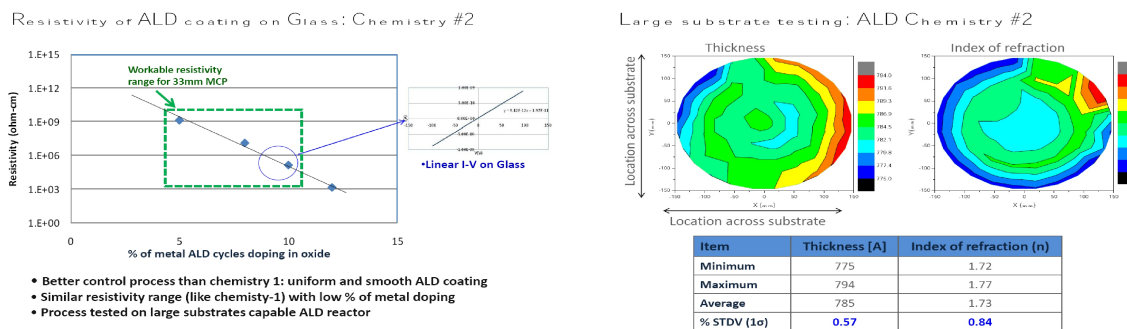


Figure 15: Left: The resistivity curve of one of these new formulations. Resistivity is plotted versus the number of metal cycles. Right: Measurements of uniformity on a large substrate, one of the first steps towards scale-up.

Knowledge Gained

New formulations of resistive coatings for MCP's with higher reproducibility (and hence higher yields), better control of resistance range, and better thermal behavior than AZO.

4.8 Technical Achievement 8: Modeling of Emissive Coatings for Micro-channel Plates

Theory-driven design could allow tailoring the secondary electron emission (SEE) properties inside the pores to allow discrete dynode structures for higher gains, better stability, faster timing or better single-photon resolution, for example. Figures 16 and 17 show the results of simulation of the interaction of electrons in the walls of the pores of the MCP plates for Al_2O_3 and MgO . The simulation effort is working closely with the program of MCP measurements to improve the input parameters.

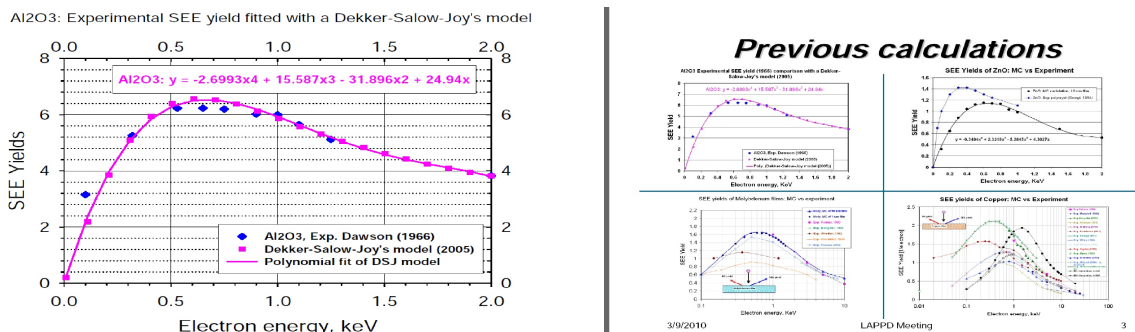


Figure 16: Left: A comparison of measurements of secondary emission in Al_2O_3 with a theoretical model. Right: Comparison with measurements in ZnO, Molybdenum, and Copper.

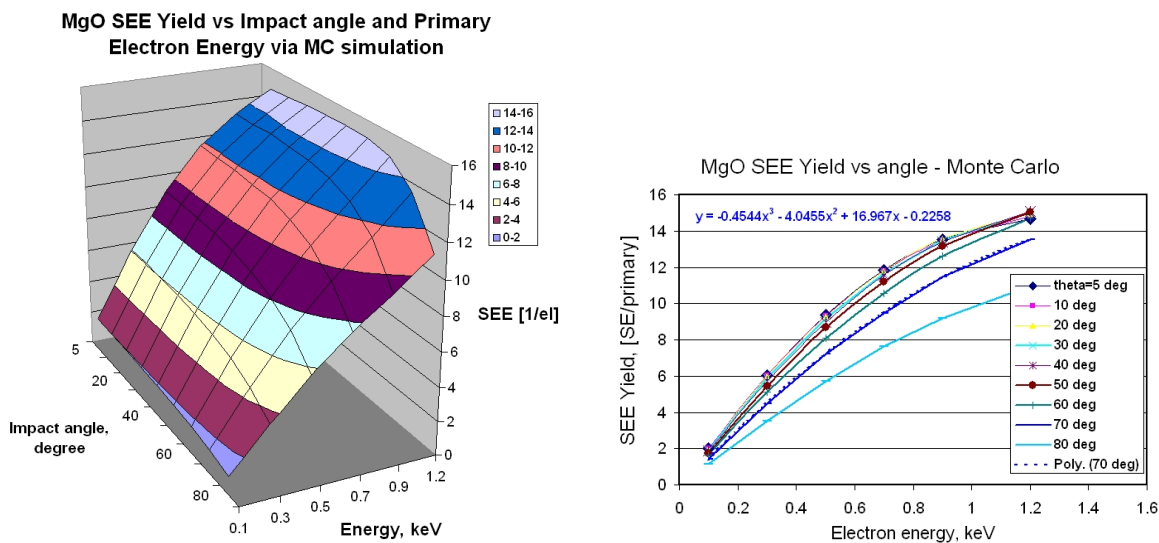


Figure 17: Left: The simulated secondary emission yield as a function of angle and energy in MgO Right: The same as a 1-dimensional plot.

Knowledge Gained

A parameterized set of SEE-yield dependencies on two variables- the electron energy and incident angle. The method has been calibrated on measurements on Mo, Cu, and Au (See Section 4.9), and can be used in the selection of emitting materials and MCP simulation.

4.9 Technical Achievement 9: Characterization Facility Construction and Measurement of Secondary Emission

The left-hand panel of Fig. 18 shows the dedicated LEED/XPS/UPS [3] secondary emission measurement and material characterization facility. Calibration measurements on gold are shown in the right-hand panel.

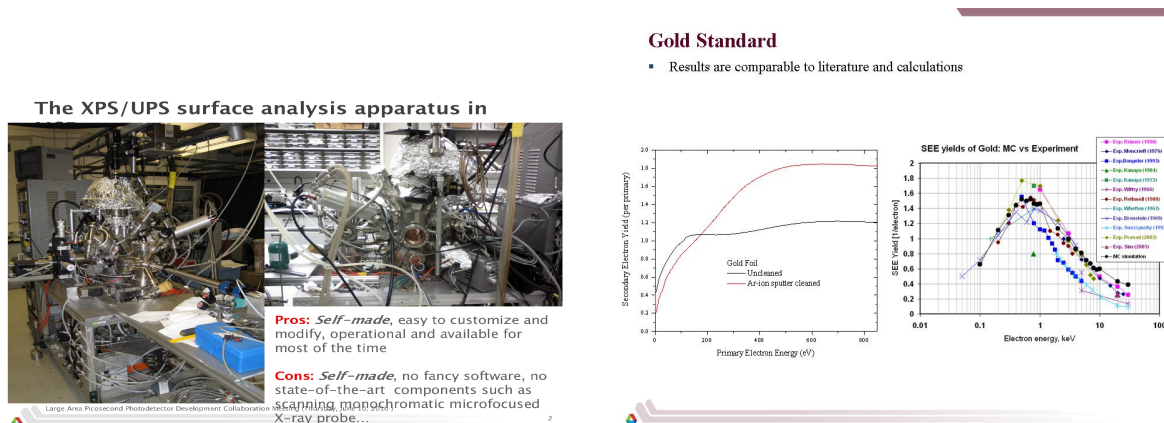


Figure 18: Left: the dedicated XPS/UPS secondary emission measurement and material characterization facility. Right: Calibration measurements on gold.

A comparison of UPS [3] measurements in MgO and Al₂O₃, two of the leading candidates for secondary emitting MCP coatings is shown in Figure 19; The right-hand panel shows a comparison of secondary emission vs incident electron energy in MgO and Al₂O₃. The voltage across the photocathode-MCP1 gap can be set to produce primary electrons with energies above 200 eV, where MgO has a significantly higher SEE than Al₂O₃

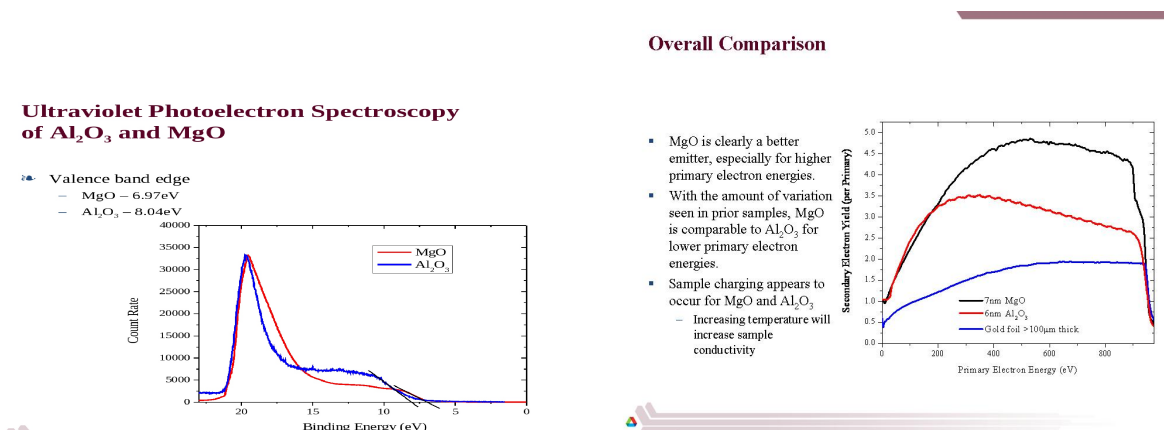


Figure 19: Left: Comparison of UPS measurements in MgO and Al₂O₃, two of the leading candidates for secondary emitting MCP coatings; Right: A comparison of secondary emission vs incident electron energy in MgO and Al₂O₃.

Knowledge Gained

A dedicated facility for measurement of low-energy secondary emission yields has been constructed and calibrated. Secondary emission spectra vs energy have been measured for candidate materials for ALD functionalization of MCP's. A cross-calibration has been made between the Arradiance and ANL Al₂O₃ secondary emission coatings. Higher gains at the first strike can be achieved with MgO than with Al₂O₃.

4.10 Technical Achievement 10: Construction of Test Facilities at both SSL and ANL

Extensive testing of functionalized 33-mm glass substrates has been done at both the Space Science Lab, UC Berkeley (SSL), focused on gain, uniformity, and aging using optical light sources, and Argonne, focused on timing using fast lasers. Figure 20 shows some of the new test facilities at SSL (left-hand panel). Also shown are test results obtained at the facility at SSL of a glass substrate functionalized with ALD at Arradiance (right-hand panel).

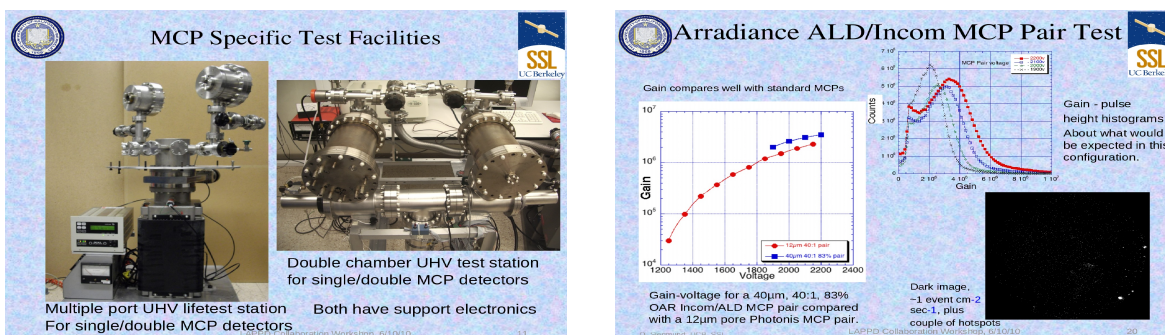


Figure 20: Left: Test facilities at the Space Science Lab, UC Berkeley. Right: Test results obtained at the facility at SSL of a glass substrate functionalized with ALD at Arradiance.

The new test MCP facility at the APS at ANL is shown in Figure 21 (left-hand panel). Also shown are measurements of pulse widths and rise-times using glass substrates functionalized with ALD at ANL and the femto-second laser (right-hand panel).

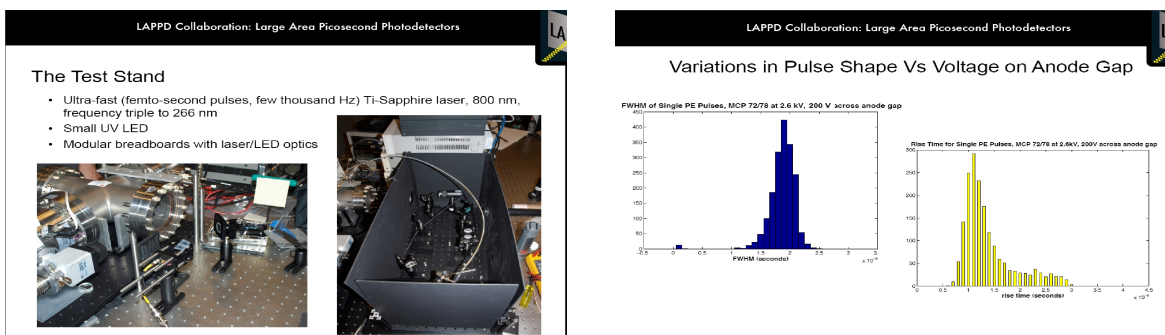


Figure 21: Left: New test facilities at ANL. Right: Measurements of pulse widths and rise-times using glass substrates functionalized with ALD at ANL and the femto-second laser

Knowledge Gained

At SSL a suite of test facilities has been constructed and commissioned for measurement of gain, uniformity, and aging. At ANL a vacuum test stand interfaced to a femto-second laser has been constructed and commissioned. Anodes with strip-lines provide a high bandwidth analog readout to a fast digital scope. Both photocathodes and functionalized MCP substrates can be measured with high time and space resolution.

4.11 Technical Achievement 11: Measurement of 2-psec Relative Time Resolution and 100 μm Space Resolution with Transmission-Line Readout coupled to an MCP-PMT

A test setup using a commercial Planacon 1024-anode MCP-PMT coupled with silver-loaded epoxy to a transmission-line printed circuit card constructed to match the anode spacings is shown in the left-hand panel of Fig. 22. The right-hand panel shows results taken with the ANL picosecond laser test-stand and a 40 GSsample/sec Tektronix oscilloscope. A resolution of 2 psec in time between one end of the strip line and the other is measured, corresponding to 100 micron space resolution.

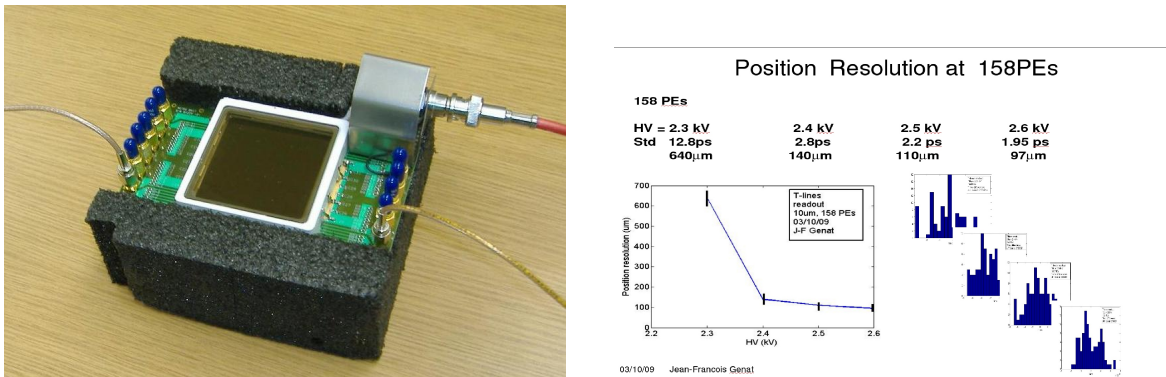


Figure 22: Left: A commercial Planacon 1024-anode MCP-PMT coupled with silver-loaded epoxy to a transmission-line printed circuit card. Right: Results taken with the ANL picosecond laser test-stand and a 40 GSsample/sec Tektronix oscilloscope. A resolution of 2 psec in time between one end of the strip line and the other is measured, corresponding to 100 micron space resolution.

Knowledge Gained

Even before optimization and with klutzy (i.e. inductive) anodes, micro-channel plates with strip lines are capable of psec time and 100-micron space resolutions.

4.12 Technical Achievement 12: The Development of 8"-square Glass-Capillary Plates for LAPPD MCP-PMT's by Incom, Inc (Charlton Mass.)

Fig. 23 shows a micro-photograph of an Incom 20 micron capillary substrate. This plate has an open-area-ratio (OAR) of $\sim 65\%$ and a length/diameter (L/D) ratio of 60. The plates are quite robust, as the borosilicate glass is much harder than the commercial lead glasses, and also has not been chemically treated. Incom has made substrates with OAR's up to 83%. The substrates have been shown to provide adequate uniformity and noise, as well as attractive gain and aging characteristics.

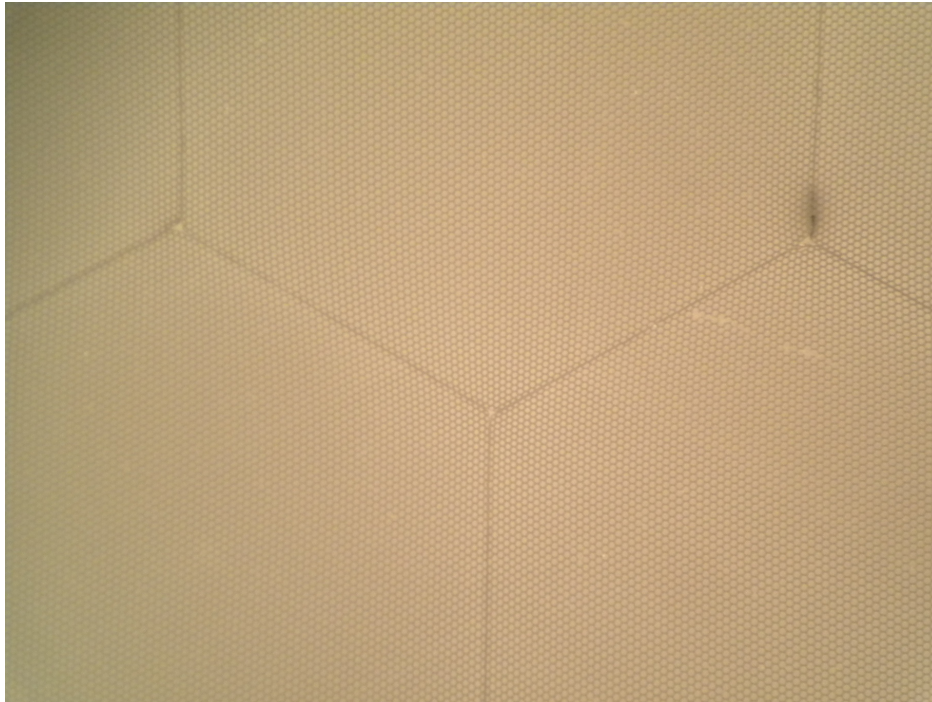


Figure 23: A micro-photograph of an Incom 20 micron capillary substrate. This plate has an open-area-ratio (OAR) of $\sim 65\%$ and a length/diameter (L/D) ratio of 60.

Knowledge Gained

Inexpensive glass capillary arrays can be fabricated at a quality and volume such that they can be used as homogeneous fine-grained amplifying structures in large-area arrays of photo-detectors.

4.13 Technical Achievement 13: Steps in the Development of Nano-structured Anodic Aluminum Oxide Substrates

Anodic Aluminum Oxide (AAO) substrates are a possible alternative to glass capillary substrates. Synkera Technologies has demonstrated new processes for high-voltage anodization with improved pore uniformity and alignment. Pore period >1 micron, pore diameter of 0.5 micron, thickness of 0.02 - 0.1 mm and L/D of 40-200 have been demonstrated in small samples (Figure 24, Left). Equipment, tooling and processes, including etching and annealing, have been scaled up and substrates in the 33 mm format have been delivered to both ANL and Arradance for ALD functionalization (Figure 24, Right).

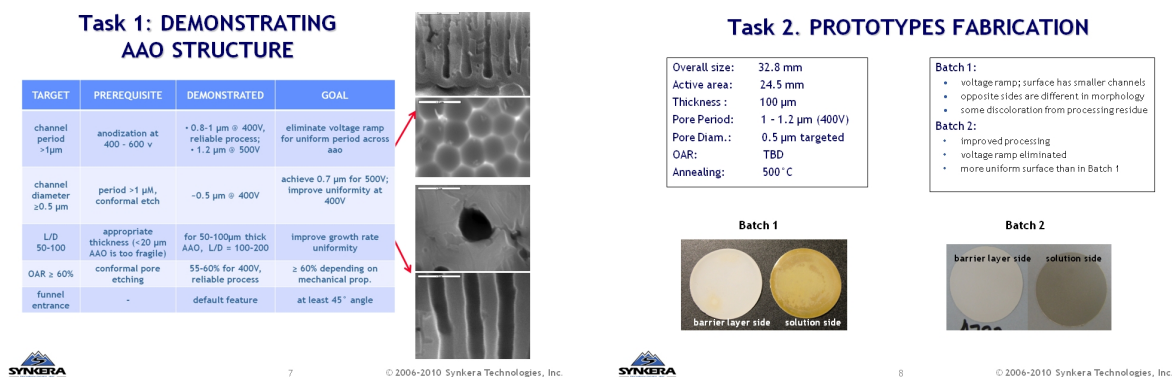


Figure 24: Left: The AAO pore structure. Right: Synkera MCP substrate prototypes.

At Argonne a new electro-polishing procedure has been developed. Using a photo-lithographic patterning technique and improved wet etching process, 1.6 cm-square plates with an L/D ratio of over 15 have been fabricated. Open area ratios (OAR) up to 60% have been demonstrated. Figure 25 (Left) shows the front-side of an AAO plate with 28-micron pores. Note the funnel-shaped openings. Right: The back-side of the plate with 26 micron pores.

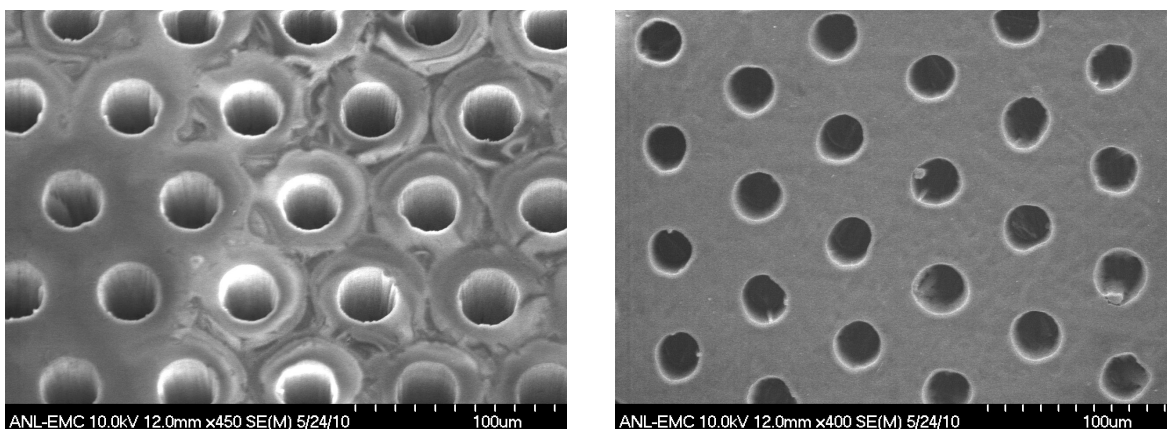


Figure 25: Left: The front-side of an AAO plate with a pore-size of 28 microns. Note the funnel-shaped openings. Right: The back-side of the plate; the pore size is 26 microns.

Knowledge Gained

Intrinsic AAO channels with diameter and L/D ratios close to the targeted values for small pore MCP's are possible. The alternative micro-machined approach enables achieving pores with channel diameter, L/D, and OAR closer to conventional MCP values. Funnel openings are possible with AAO.

4.14 Technical Achievement 14: Simulation-based Design of MCP's and Validation by Test Measurements

The performance of MCP-PMT's depends on many parameters; a traditional program of optimization by experimental trial-and-error and intuition cannot explore the full space in any conceivable time or funding profile. Simulation validated by experiment in a coarse sampling of the space can provide essential guidance towards optimization.

The left-hand panel of Fig. 26 shows a simulation of the electric field lines at the entrance to an electrode-plated MCP plate. The first strike is a strong determinant of the time resolution (time-transit spread, TTS) and single-photon charge distribution resolution; optimization of the geometry and materials at the entrance to the pore is consequently high-payoff. Subsequent evolution of the shower in the pore is shown in the right-hand panel for different pore angles.

Spoiled end. Color: field angle

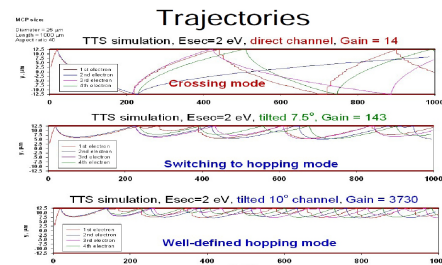
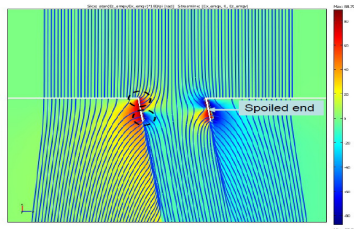


Figure 26: Left:Simulation of the electric field lines at the entrance to an electrode-plated MCP plate. Right: Subsequent evolution of the shower in the pore for different pore angles.

Novel geometries can also be explored before investing resources in realizing them. A geometry with a funnel opening to the pore on which the photocathode is deposited would have many advantages: the reflective photocathode could be thicker and so would have higher QE; the photocathode is shielded from ion feedback that shorten lifetimes; a larger open-area-ratio could be achieved as the funnels would cover the surface; extraordinary time resolutions might be achieved as the first gap is crossed by a photon rather than a slow electron, and the path length from first-strike to shower is on the order of 10 microns rather than a millimeter.

Figure 27 shows a simulation of a funnel pore.

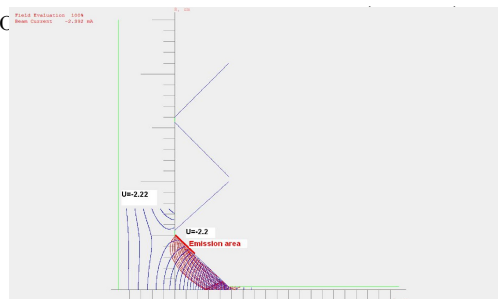


Figure 27: Simulation of electron trajectories (in red) for a funnel pore. The pore extends horizontally to the right; the photocathode surface is the vertical line on the left.

Knowledge Gained

A sophisticated tool for optimization of timing, efficiency, pulse-height distribution, and geometry has been created and is being used to optimize ALD-functionalized glass substrate MCP plates.

4.15 Technical Achievement 15: Understanding Timing Information Content of MCP-PMT Signals: Theory and Measurements

In the LAPPD large-area design both the position of the particle (photon or charged particle) and the time of arrival are measured using the digitized time of the pulses at the two ends of the transmission lines (See Section 4.4). The space and time resolutions thus depend on the time resolution of the signal processing.

In a previous publication we have shown detector time-resolution depends on three parameters: analog-band-width (i.e. rise-time), signal-to-noise, and photon statistics. In order to extract the maximum amount of information from the MCP-PMT signals, but not build in unnecessary expense and complexity, one has to understand the frequency spectra of both signal and noise. The left-hand panel of Figure 28 shows the frequency signal and noise content of the MCP-PMT signals from a commercial module.

In the ANL laser test-stands we measure analog bandwidths of several gigahertz for these MCP-PMTs. Preserving this bandwidth while providing an economical construction has been seen as a major challenge from the inception of this project. The right-hand panel of Figure 28 shows measurements made with the ANL laser test-stand on a Planacon MCP coupled with a 50-ohm transmission-line PC board, showing that a faster sampling rate gives better time resolution, as predicted.

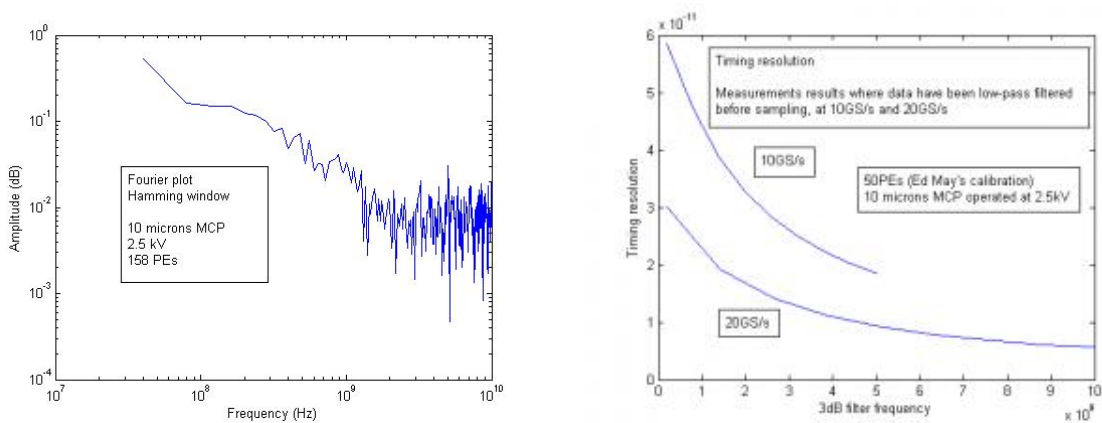


Figure 28: Left: The frequency signal and noise content of the MCP-PMT signals from a Planacon 10-micron pore MCP-PMT. Right: measurements made with the ANL laser test-stand on a Planacon MCP coupled with a 50-ohm transmission-line PC board, showing that a faster sampling rate gives better time resolution, as predicted.

Knowledge Gained

Understanding of pulse formation, transmission, and impedance matching in strip-line transmission lines. Optimization of matching the analog-band-width of the transmission line construction and ASIC input structures to the MCP-PMT signal in the frequency domain.

4.16 Technical Achievement 16: Design, Fab and Testing of a Waveform Sampling ASIC in the 130nm IBM 8RF Process

We have acquired and commissioned the IBM 8RF Cadence ASIC design kit from CERN. A first 4-channel waveform chip was submitted and tested with qualified success. The chip contained test structures as well as four channels of sampling. The ramp, ring oscillator, and sampling cells on the chip worked, but the chip did not function as a wave-form sampler. The left-hand panel of Figure 29 shows the Psec-1 chip in a probe station. The right-hand panel lists the improvements implemented in the second chip, Psec-2.

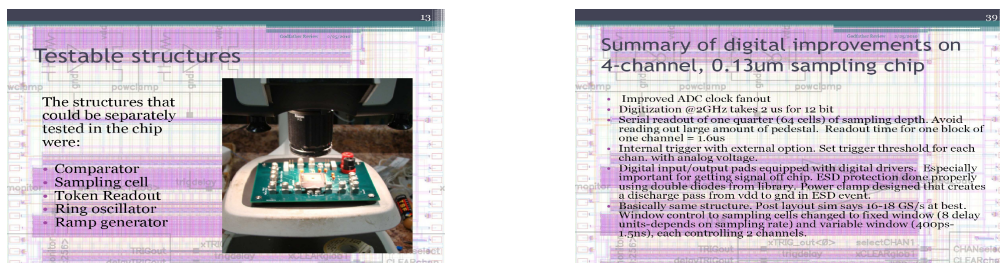


Figure 29: Left: The Psec-1 chip in a probe station. Right: Improvements implemented in the second chip, Psec-2.

The left-hand panel of Figure 30 shows a picture of the next sampling ASIC implementing the above improvements, Psec-2. This chip arrived from the foundry on June 17, 2010. The right-hand panel shows the ring oscillator structure on the chip. In the short time we have had it we have tested the analog wave-form sampling with success. Further testing continues.

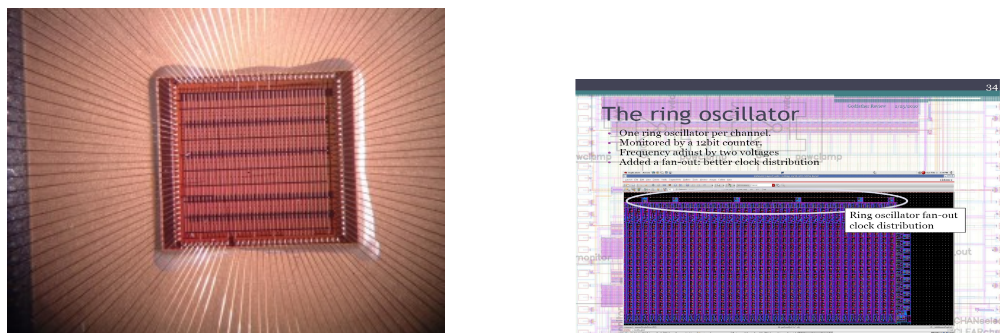


Figure 30: Left: The Psec-2 ASIC received from MOSIS June 17th. Right: The ring oscillator structure on the chip

A third chip consisting of test structures containing advanced features we may want to implement in a future sampling chip has just been submitted to MOSIS, this time through CERN. The Hawaii group has implemented a charge sensitive amplifier, delay lines, ring-oscillators, a D-flip-flop and a more advanced sampling cell array. Chicago has implemented transmission line structures, phase detectors, charge pumps, and a PLL, and a ring-oscillator and divider.

Knowledge Gained

Design of the first waveform sampling chip in 130nm. Expertise in the Cadence 8RF Design Kit, Assura DRC, Calibre DRC, and Assura LVS, and MOSIS submission procedures. Acquisition and commissioning of psec diagnostic tools.

4.17 Technical Achievement 17: Design of Integrated Analog and Digital Readout for the 16" by 24" Glass Photodetector Supermodule

The transmission line structures consist of the 9" top trace as the anode strips inside the glass tile, which form the DC ground, and a 27" bottom trace card as the tray. The transmission line strips go directly into the waveform sampling ASICs on small cards, the Analog Card, soldered to the long bottom trace card. The output of the ASICs is transferred by connector or cable (depending on the application) to the Digital Card. Figure 31 (Left) shows prototypes of the Analog and Digital Cards.

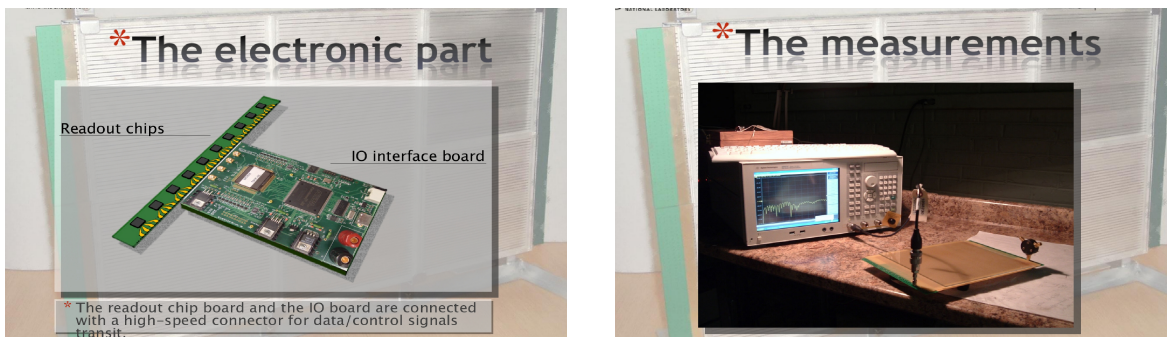


Figure 31: Left: Prototypes of the Analog and Digital Cards. Right: The test setup for measuring analog bandwidth and impedance matching.

The test setup for measuring analog bandwidth and impedance matching is shown in the right-hand panel of Figure 31. Measurements are compared with simulation using HFSS [4], as shown in the left-hand panel of Figure 32. The measured response is shown in the right-hand panel of Fig. 32.

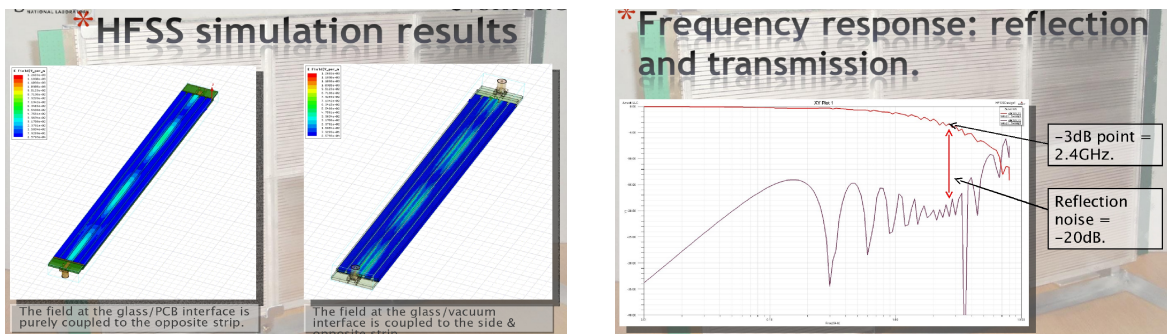


Figure 32: Left: Measurements of the transmission lines are compared with simulation using HFSS. Right: The measured response versus frequency.

Knowledge Gained

The frugal transmission-line structures screened onto glass or on single-sided PC cards have bandwidths in the 2.5 GHz range, well-matched to the MCP-PMT signals and the waveform sampling ASICs. Modeling with Ansoft software gives good agreement with measurements, meaning that we can predict.

4.18 Technical Achievement 18: Identification of Photocathode Candidate Materials, Techniques, and Facilities

An extensive effort including workshops and collaborative efforts has been started to identify photocathode materials amenable to higher performance and/or more economical assembly. Figure 33 shows a table of the main candidates for photocathodes for large-area detectors, multi-alkali, GaAs-based, and GaN-based.

Why are we Planning a Large Cathode Effort?

- Multi-Alkali seems to have perfect cathode properties
- But
 - Little understanding
 - Small community
 - No developed industry
 - Problems with mass-production
- Existing III-V cathode have not the right properties
- But
 - Excellent understanding
 - Large community
 - Excellent developed industry
 - Easy mass-production

	Property	Multi-Alkali	GaAs-based	GaN-based
Photocathode Properties	Wavelength response (typical)	150nm-500nm	450nm-850nm	100nm-350nm
	Typical efficiency	20%	20%	30-40%
	Maximum efficiency	50%	60%	80%
	Wavelength tunability	low	large	Very high
	Dark current	~100cps/cm2	~10000cps/cm2	~100cps/cm2
Growth properties	Single crystal substrate	no	yes	yes
	Easy scalable	No	yes	yes
	Large production volume possible	No	Yes	Yes
	Prefabrication possible	No	Yes	Yes
	Temperature sensitive	High	Medium	Medium
	Existing industry	No (besides night vision / small area)	Yes (foundries available)	Yes (foundries available)
Basic Physics	Good understanding	No	Yes	Yes
	Microscopic understanding of growth	No	Yes	Yes
	2-D Fabrication tools	No	Yes	Yes
	3-D Fabrication tools	No	Yes	Some
	Theoretical description	No	Yes	Yes
	Band-structure engineering	No	Yes	Yes

Figure 33: The three dominant families of candidate photocathodes for very large area arrays. Very high quantum efficiencies have been achieved in all three (shaded in gold), well above the commercial norm. Each of the families has significant downsides, as shown in red.

Figure 34 shows a ‘road-map’ of the people and places collaborating on photocathodes within the LAPPD Collaboration. There is a separate collaborative effort with BNL, focused on materials aspects of multi-alkali photocathodes. We note that the two complementary light sources at ANL and BNL and the charged particle test beam at Fermilab provide access to the full input signal spectrum.

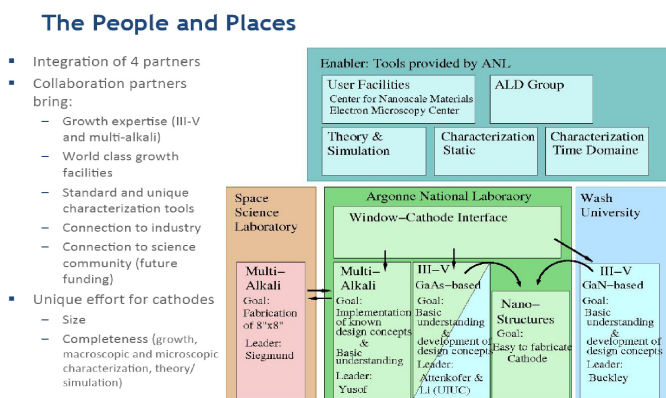


Figure 34: A ‘road-map’ of the people and places collaborating on photocathodes within the LAPPD Collaboration.

Knowledge Gained

Photocathode materials have been evaluated in terms of potential for QE, wavelength tuning, robustness and stability, and manufacturability.

4.19 Technical Achievement 19: Coordination of Existing Photocathode Facilities and Design of a New Dedicated Photocathode Growth/Characterization Facility at ANL

Figure 35 (left-hand panel) shows the design of a dedicated facility for the growth and characterization of multi-alkali, III-V, and nano-structured photocathodes. This will be installed in the MSD Division at ANL in close proximity to the existing characterization facilities. The right-hand panel shows the growth and characterization facility used for GaN at the University of Washington.

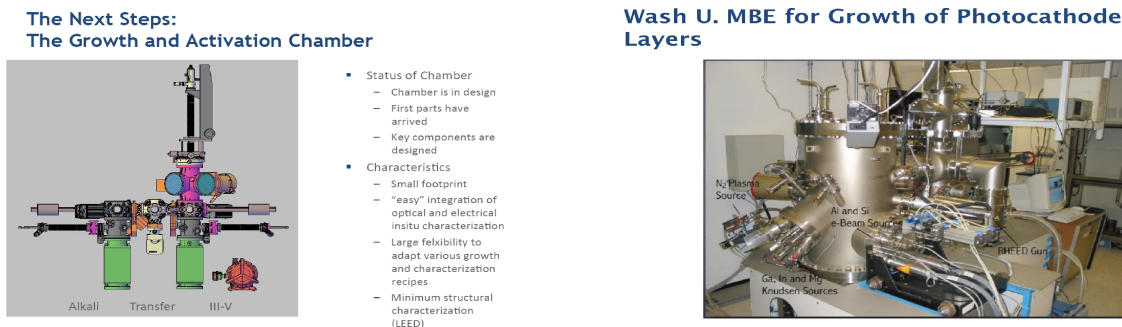


Figure 35: Left: The design of a dedicated facility for the growth and characterization of multi-alkali, III-V, and nano-structured photocathodes. Right: The growth and characterization facility used for GaN at the University of Washington.

A sophisticated facility is also being used at the University of Illinois, Urbana, for exploration of GaAs-based and nano-structure photocathodes. A surface in GaAs showing a regular set of plateaus grown in the UIUC facility is shown in Figure 36

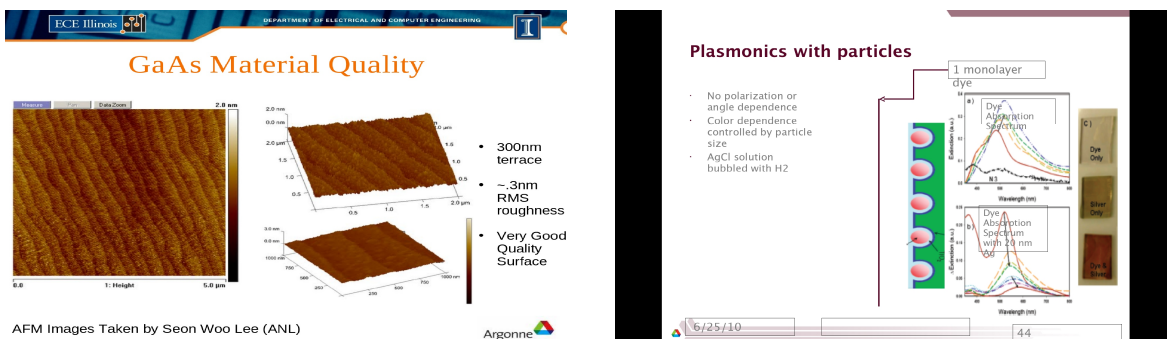


Figure 36: Left: A surface in GaAs showing a regular set of plateaus grown in the UIUC facility. Right: A proposed plasmonic photocathode, tunable by wavelength, based on easily deposited metalized nano-arrays.

Knowledge Gained

A photocathode initiative encompassing inter-disciplinary expertise, condensed matter physics knowledge, and sophisticated facilities has been created. A plan for growth and characterization of multi-alkali, III-V, and nano-structure materials has been made, and hopefully knowledge will be gained.

4.20 Technical Achievement 20: Initial designs and cost estimates for the glass-phototube fabrication facility.

The newly-evolved tile-tray design is built on an 8”-square vacuum tube, the ‘Tile’, to achieve a large area with a common readout. We are now in a position to design the ‘Tile Factory’. We have located lab space at ANL, and made initial trials of the assembly steps. Figure 37 shows a work-flow plan for initial preparation (Left), and a proposed layout for the tile assembly (right). Visits to learn assembly flow have been made to Photonis (Brive), Burle (Lancaster), UC Davis and UC Berkeley, Siegmund Scientific (Walnut Creek), and the CERN photocathode lab.

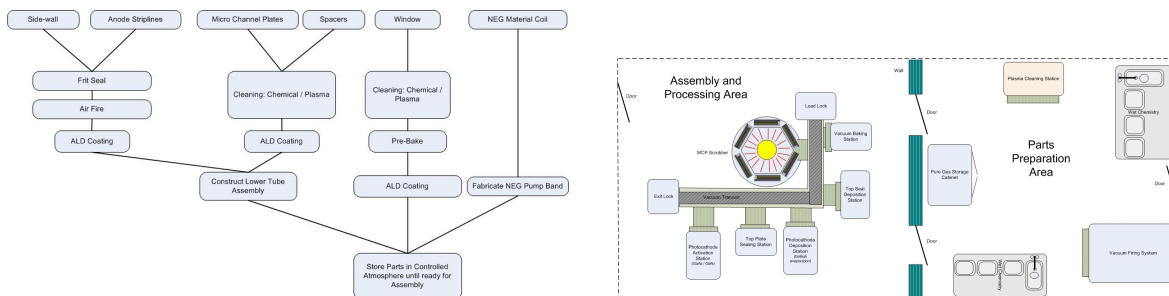
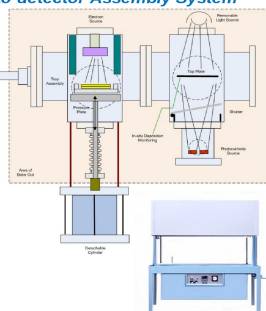


Figure 37: Left: work-flow plan for initial preparation. Right: A proposed layout for the Tile Factory tube assembly facility at ANL.

The left-hand panel of Figure 38 shows an initial design for photocathode deposition based on the steps above. The right-hand panel shows photomultiplier assembly stands visited at Burle in Lancaster, Pa.

Photocathode Deposition & Photo-detector Assembly System

- Dual chamber manual process system
- Deposition Chamber
 - Ability to degas sources without contaminating other parts.
 - Once shutter is open, it will act a shield for the other parts to prevent accidental deposition
 - There will be the ability to monitor the deposition through current measurement while the photocathode is being illuminated
- Scrubbing and Bonding Chamber
 - This will house the electron source to scrub the MCP.
 - The detachable cylinder will apply the force necessary to affect a pressure indium seal.
- System will be bakeable to 350 C



Industrial Photo-detector Processing System



Figure 38: Left: An initial design of a tile fabrication facility. Right: Photomultiplier assembly stands visited at Burle in Lancaster, Pa.

Knowledge Gained

Procedures for pre-cleaning assembly of sealed glass tubes. Preliminary estimates of facility through-put and costs. Industry contacts.

5 Year 1 Milestones

5.1 Section A: Schedule or Milestone Requirements

5.1.1 A-1: Identify and characterize Photo-electron Emission (PE) properties of materials for photocathode development.

Done. (See Technical Achievement 4.18 above.)

5.1.2 A-2: Demonstration of amplification with gain ≥ 300 with an atomic layer deposition (ALD)-functionalized micro-channel plate.

Done (See Technical Achievement 4.1 above.)

5.1.3 A-3: Achieve a differential time resolution ≤ 10 picoseconds and a space resolution ≤ 1 mm in vacuum with a 50-ohm transmission-line anode suitable for multi-photoelectron high-precision applications.

Done. (See Technical Achievement 4.11 above.)

5.2 Section B: Performance Outcomes and Measures

5.2.1 B-1: Upgrade existing collaboration vacuum-transfer facilities to match the 8"-square module assembly.

In progress. The completion of this task was slowed by the evolution and simplification of the ceramic module design during the year, and the delay in getting funding to SSL as described in Milestone B-4 below. (See Technical Achievement 4.3 above.)

5.2.2 B-2: A design, including costing and interfacing with vendors of production sealed-glass tubes, for a vacuum-transfer/assembly facility for the 8"-square module assembly.

Finished, but restarted and presently evolving due to the new Tile-Tray design allowing a 16" by 24" SubModule as our basic photo detector with substantial economies per photo-area (See Technical Achievements 4.4 and 4.20 above.)

5.2.3 B-3: Design a prototype-type 2-channel ASIC with sampling rate ≥ 20 GSample per second, analog bandwidth ≥ 1.5 gigahertz, and a capacitor-sampling chain and timing-generator blocks.

Done. (See Technical Achievement 4.16 above.)

5.2.4 B-4: Demonstration of an operational 8"-square photocathode.

We have requested a 6-month extension as the funding for the SSL effort was not available to order the vacuum tank and other necessary items until March 2010. All equipment is either on order or in house, and smaller photocathodes have been made and demonstrated to work as part of the program.

5.2.5 B-5: Demonstration of a vacuum seal of the 8”-square window to the body.

Done as written. The seal we have made and tested will work for high-temperature photocathodes such as III-V (GaAs and GaN families), nano-structured photocathodes, and the evaporated metal photocathodes appropriate for some calorimetry (See Technical Achievement 4.5 above). A low temperature Indium cold-seal, such as we have learned is technically feasible and is mass-produced in industry, is in progress.

6 Summary and Outlook

In this first year we have made significant progress in the technical areas that lie on the critical path to economical large-area, fast, planar photo-detectors, and have laid the groundwork for the next steps. The next year should see a continuation of laying a deeper understanding and the ramp-up of the photocathode growth and characterization program at Argonne, and the construction of the Tile Factory, which includes photocathode deposition for prototype production tiles.

References

- [1] A list of personnel and individual contact information is available at <http://psec.uchicago.edu/people.php>.
- [2] Paul Horn, VP for Research, IBM Corporation
- [3] AZO is the acronym for Aluminum Zinc Oxide; LEED for Low-Energy Electron Diffraction; XPS for Xray Photoelectron Spectroscopy; UPS for Ultraviolet Photoelectron Spectroscopy.
- [4] HFSS is a 3D Full-wave Electromagnetic Field Simulation from Ansoft Corporation.